applied sciences

MDPI

Article

Synthesis and Selected Properties of Ester Elastomer Containing Sorbitol

Marta Piątek-Hnat [1,*], Kuba Bomba [1] and Jakub Pęksiński [2]

[1] Faculty of Chemical Technology and Engineering Piastów Ave. 42, West Pomeranian University of Technology, 71-065 Szczecin, Poland; bk34688@zut.edu.pl
[2] Faculty of Electrical Engineering, Sikorskiego Ave. 37, 71-313 Szczecin, Poland; jakub.peksinski@zut.edu.pl
* Correspondence: marp@zut.edu.pl

Received: 1 February 2020; Accepted: 23 February 2020; Published: 29 February 2020

Abstract: The aim of this work was synthesizing ester elastomers, using sorbitol as a monomer obtainable from renewable sources. Three polymers were synthesized, utilizing three different polycondensation times. Their mechanical and thermal properties were examined and compared. Poly(sorbitol sebacate-co-butylene sebacate) elastomers were synthesized as a result of polycondensation reaction, using sebacic acid, butylene glycol and sorbitol as monomers. Resulting materials had good mechanical properties and a cross-linked structure. Such elastomers are susceptible to hydrolytic degradation which has been confirmed in earlier studies. This paper shows that the material synthesized utilizing a 3.5 h polycondensation time has the most desirable mechanical and thermal properties, and the reaction is characterized by the highest degree of conversion of substrates.

Keywords: elastomers; polycondensation; sustainable sources; biodegradable material; material properties

1. Introduction

Due to environmental concerns, obtaining biodegradable polymers synthesized by utilizing monomers possible to acquire from renewable sources became a topic of interest among various researchers. One such group of materials is sugar alcohol-based polymers. The most researched materials of this type are glycerol-based. They have been proven to have many possible biomedical applications [1–10]. Various polymers obtained using sorbitol as monomers include sorbitol-based terpolyesters [11] and biocompatible polymers based on sebacic acid and different sugar alcohols, including sorbitol [12]. A biocompatible polymer based on sorbitol and sebacic acid was also obtained [13]. Copolymers with succinic acid, sorbitol and different diols were also obtained and tested [14]. A sorbitol-based polymer with citric and sebacic acid as monomers and its biodegradability was also described in earlier work [15]. Sorbitol can also be used as a chain extender in self-healing polyurethanes [16]. Biodegradable composites with hydroxyapatite in a poly(sorbitol sebacate malate) matrix can also be obtained [17].

Various examples of sugar alcohol-based polymers have been described in the literature. Polyesters were obtained using different xylitol–sebacic acid ratios. Their properties were tested, and the elastomers have been proven to be biocompatible in vitro [18]. Xylitol-based polymers synthesized using citric and sebacic acid were obtained. Poly(xylitol-co-citrate) was then copolymerized with methacrylic anhydride. The materials have been proven to be biocompatible in vivo [19]. Copolymers with two dicarboxylic acid segments were also synthesized and tested [20]. Sugar alcohol-based polymers have also been proven to be possible to synthesize using lipase as a catalyst [21]. Exact structure of non-cross-linked poly(xylitol sebacate) has also been

determined and proven to be a linear chain. The polymer contains mostly 1,5-diacyl and 1-acyl substitutions [22]. Other interesting materials obtained using sugar alcohols include: nanocomposites of poly(mannitol sebacate) with cellulose nanocrystals which display shape-memory properties [23], poly(xylitol-co-maleate-co-PEG) hydrogel, which can be used in order to encapsulate and inject cells [24], poly(xylitol sebacate), which can be electrospun by a core-shell method in order to obtain tissue-like material [25,26], biodegradable poly(xylitol-dodecanedioic acid) with possible future tissue-engineering applications [27], polymers able to reversibly solidify and liquefy, synthesized utilizing sugar alcohol and azo compounds [28], and conetworks based on poly(lactide) and sugar alcohols as core molecules [29].

In this work we focus on obtaining three-monomer-based copolyesters and analyze how changing the polycondensation time affects the mechanical and thermal properties of resulting material. The novelty in this work is that, to the best of our knowledge, material obtained using exactly those monomers has not yet been synthesized. It is also of importance that one of the monomers used—sorbitol—can be obtained from renewable sources.

2. Material and Methods

2.1. Synthesis of Poly(sorbitol Sebacate-Co-Butylene Sebacate) (PSBS)

Sigma-Aldrich (St. Louis, MO, USA) Corporation was the purveyor of the monomers used for the synthesis. $Ti(BuO)_4$ catalyst was purchased from Fluka. The monomer ratio of sebacic acid–sorbitol–butylene glycol was 2:1:1. Synthesis of sorbitol-based ester elastomers is comprised of three stages—esterification, polycondensation and post-polymerization. In the first stage, an esterification reaction catalyzed by $Ti(OBu)_4$ occurred between sebacic acid, sorbitol and butylene glycol at 150 °C. The second stage was a polycondensation reaction in a vacuum. Post-polymerization took place in a vacuum dryer; during this step, polymers cross-linked. Polycondensation was carried out utilizing three different reaction times: 1 h (PSBS 1 h); 2.5 h (PSBS 2.5 h) and 3.5 h (PSBS 3.5 h) in order to shorten the cross-linking stage of the synthesis and to determine which resulting material had the best thermal and mechanical properties. The reaction scheme is shown in Figure 1.

2.2. Methods

2.2.1. Fourier-Transform Infrared Spectroscopy (FTIR)

In order to analyze the chemical structure of the materials, Fourier-transform infrared spectroscopy (FTIR) was used. The range of the transmission spectra recorded by the FTIR method was between 4000 and 400 cm^{-1}. The resolution used was 2 cm^{-1}. Software used to develop the test results was OMNIC 7.3 by the Thermo Electron Corporation.

2.2.2. Differential Scanning Calorimetry (DSC)

Determination of the thermal properties was performed with a differential scanning calorimetry (DSC) (Q100, TA Instruments) apparatus. The temperature range of the heating cycle was −100 to 200 °C. The heating rate used was 10 °C/min. The samples were kept in a nitrogen atmosphere. Software used to develop the test results was TA Instruments Universal Analysis 2000, 3.9a.

2.2.3. Dynamic Thermomechanical Analysis (DMTA)

In order to perform dynamic thermomechanical analysis, a DMA Q800 (TA Instruments) was used. The temperature range was −100 to 150 °C, with 1 Hz frequency. The heating rate was 2 °C/min. Software used to develop the test results was TA Instruments Universal Analysis 2000, 3.9a.

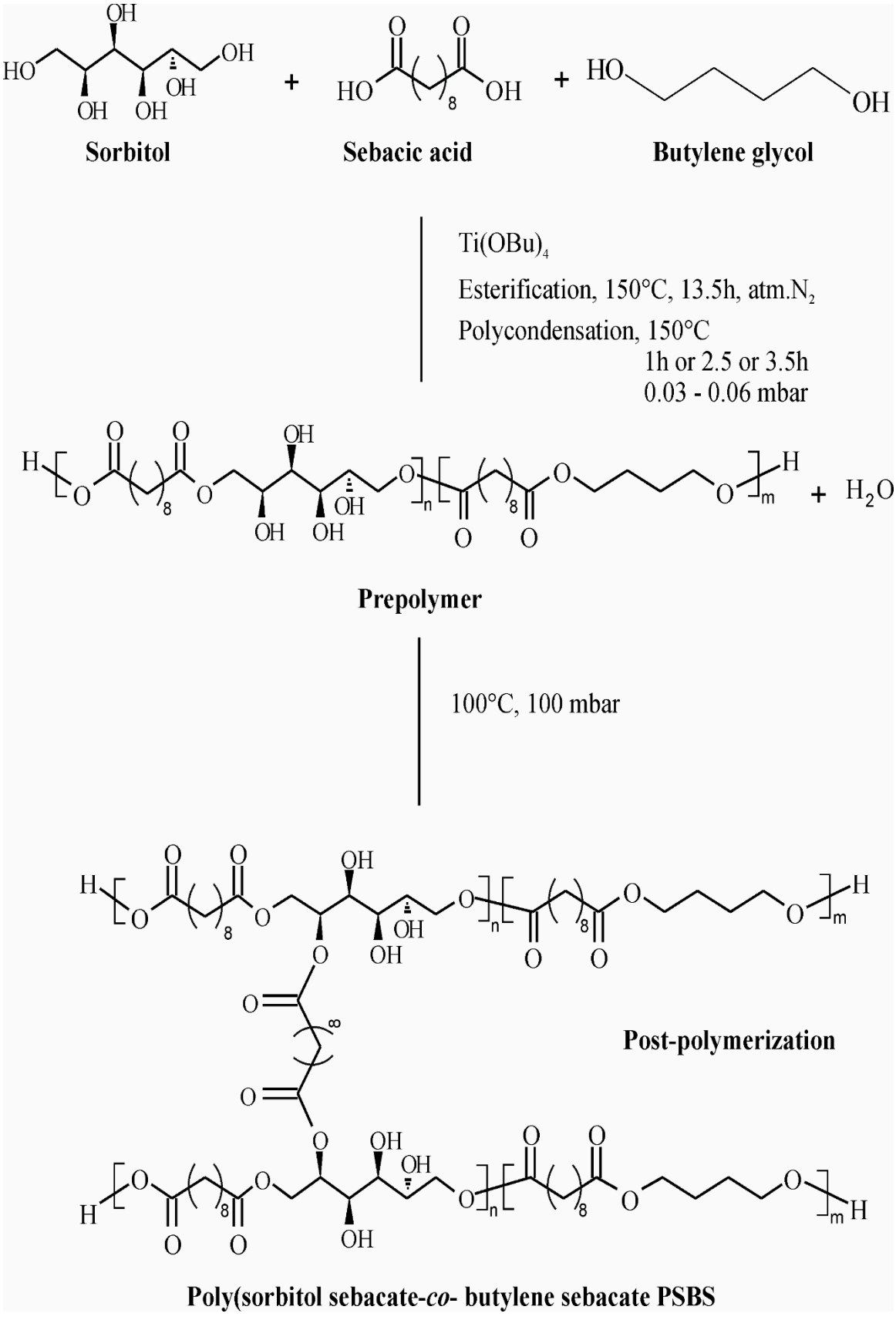

Figure 1. Scheme of poly(sorbitol sebacate-co-butylene sebacate) (PSBS) synthesis.

2.2.4. Mechanical Properties

In order to perform the mechanicals tests, an Instron 336 instrument was used. 500 N load cell was used. The tests were performed according to PN-EN-ISO 526/1:1996 standards. Crosshead speed was 100 mm/min. The temperature was 25 °C. Relative humidity was 50%.

2.2.5. Gel Fraction

In order to determine the gel fraction, the PN-EN-579:2001 extraction method was utilized. Samples of cross-linked material were used. The weight of each sample was about 1 g. A Schott crucible Type P2 was utilized. Samples were extracted with 100 cm^3 of boiling tetrahydrofuran. The extraction took 3 h. A vacuum oven was used to dry the samples. The drying process took 3 h and was performed in 25 °C. After that, the samples were dried in a desiccator. Formula (1) was used in order to calculate the gel fraction content. The mean of three measurements was used.

$$X = \frac{m_1}{m_0} 100\% \quad (1)$$

where m_0—mass of the sample before extraction, m_1—mass of the sample after extraction.

2.2.6. ^{1}H Nuclear Magnetic Resonance Spectroscopy (NMR)

In order to analyze the chemical structure of PSBS, nuclear magnetic resonance spectroscopy (NMR) was performed. The instrument used to perform the analysis was a Bruker DPX 400 MHz. A sample of PSBS at 3.5 h was taken directly after the polycondensation. The polymer sample was dissolved in deuterated chloroform ($CDCl_3$). The results were developed with MestreNova software.

3. Results and Discussion

3.1. Fourier-Transform Infrared Spectroscopy (FTIR)

FTIR spectra (Figure 2) show four peak characteristics. The peak at about 3340 cm^{-1} corresponds to intermolecularly-associated OH groups; the peak at 2900 cm^{-1} s connected to alkyl groups; the peak at about 1720 cm^{-1} can be assigned to C=O groups and the peak at about 1150 cm^{-1} is due to C-O-C groups. Intensity of the peaks attributed to C-O-C groups is increasing with the increase of the polycondensation time, indicating a higher conversion rate of the monomers.

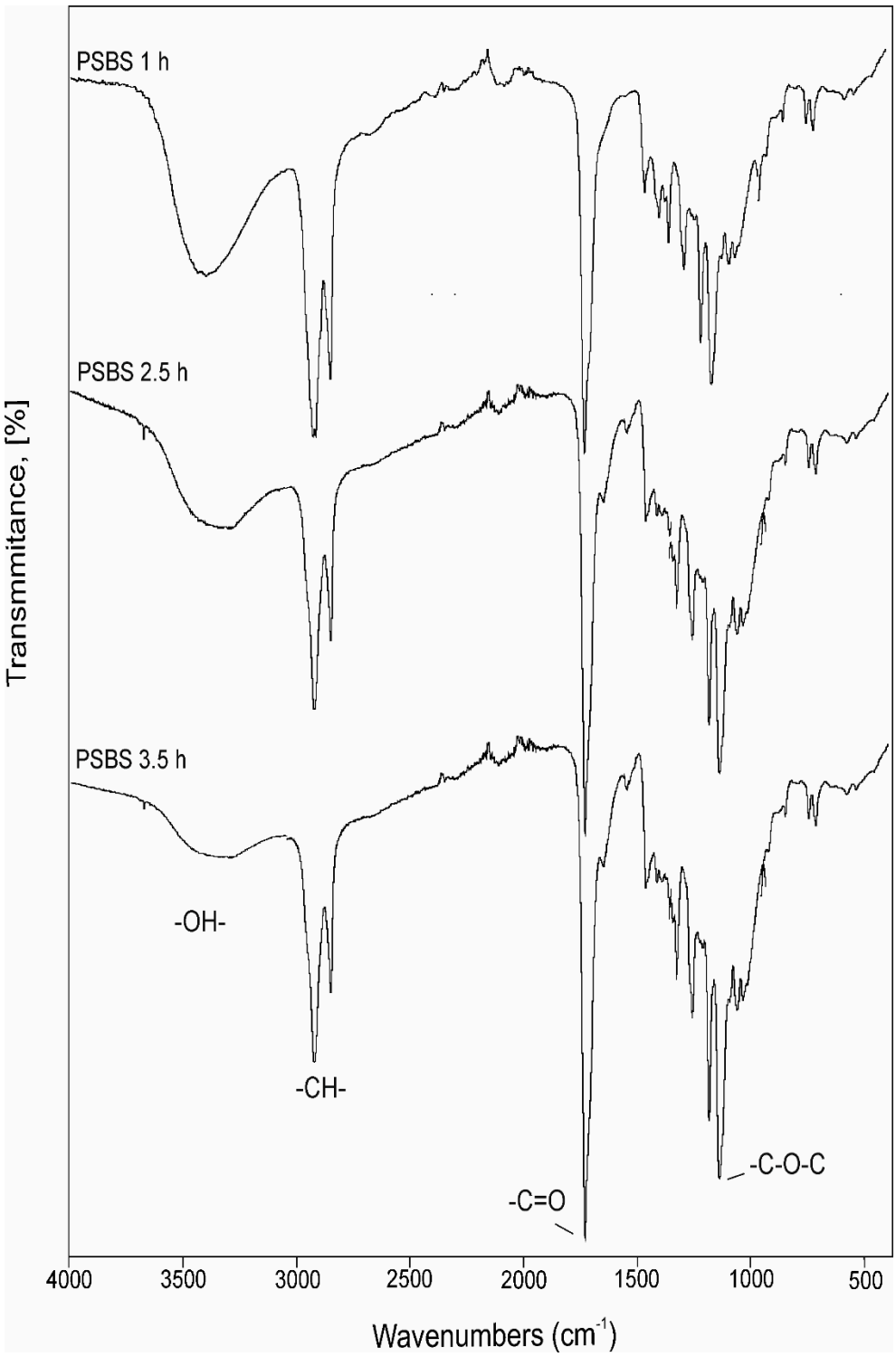

Figure 2. PSBS 1 h, PSBS 2.5 h and PSBS 3.5 h FTIR spectra.

3.2. Differential Scanning Calorimetry (DSC)

DSC was utilized in order to characterize thermal properties exhibited by PSBS elastomers obtained by utilizing three different polycondensation times (Figure 3).

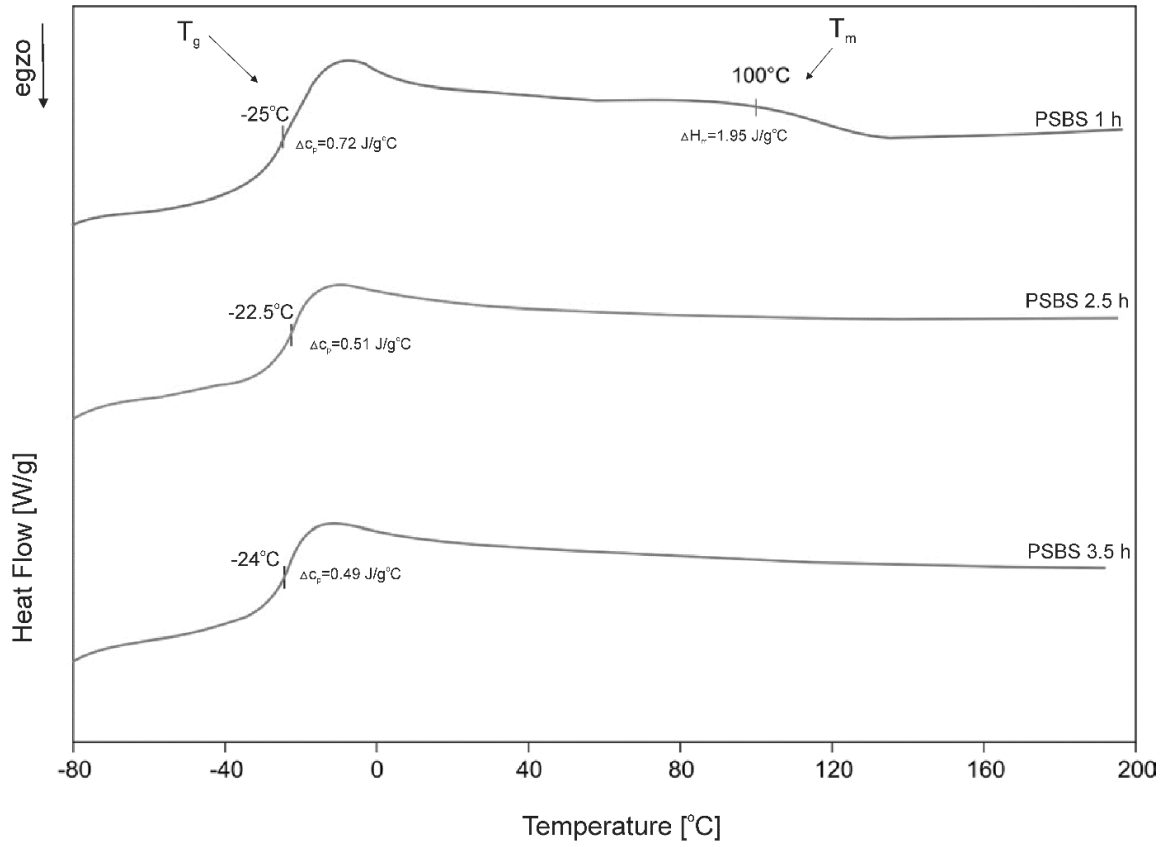

Figure 3. First-heating differential scanning calorimetry (DSC) thermograms of PSBS 1 h, PSBS 2.5 h and PSBS 3.5 h.

Glass-transition temperature (T_g) changes between materials, from −25 °C (PSBS 1 h) to −22.5 °C (PSBS 2.5 h). Change in heat-capacity during glass-transition decreases with the increase of the polycondensation time (from 0.72 J/g °C to 0.49 J/g °C). This behavior suggests an increase of cross-linking degrees and amorphous phase content and the loss of polymer-chains mobility associated with it. However, the lack of significant differences in glass-transition temperature indicates similar thermal properties of the elastomers. PSBS 1 h polymer also exhibits low-enthalpy melting, indicating small crystalline areas within amorphous polymer structures. This peak disappears with the increase of the polycondensation time due to the material being more cross-linked. The increase of cross-linking degrees and amorphous phase content, correlated with both the decrease in change in heat-capacity during glass-transition and the disappearing of the melting peak, is also confirmed by FTIR analysis. The amount of intermolecularly associated –OH groups decreases with the polycondensation time due to becoming a part of the cross-links, which causes the amount of ester groups to increase.

3.3. Dynamic Thermomechanical Analysis (DMTA)

DMTA results are shown in Figure 4. The relaxation behavior exhibited by PSBS 1 h, PSBS 2.5 h and PSBS 3.5 h was tested. Loss tangent (tan delta), loss modulus E″ and storage modulus E′ as a temperature function were measured.

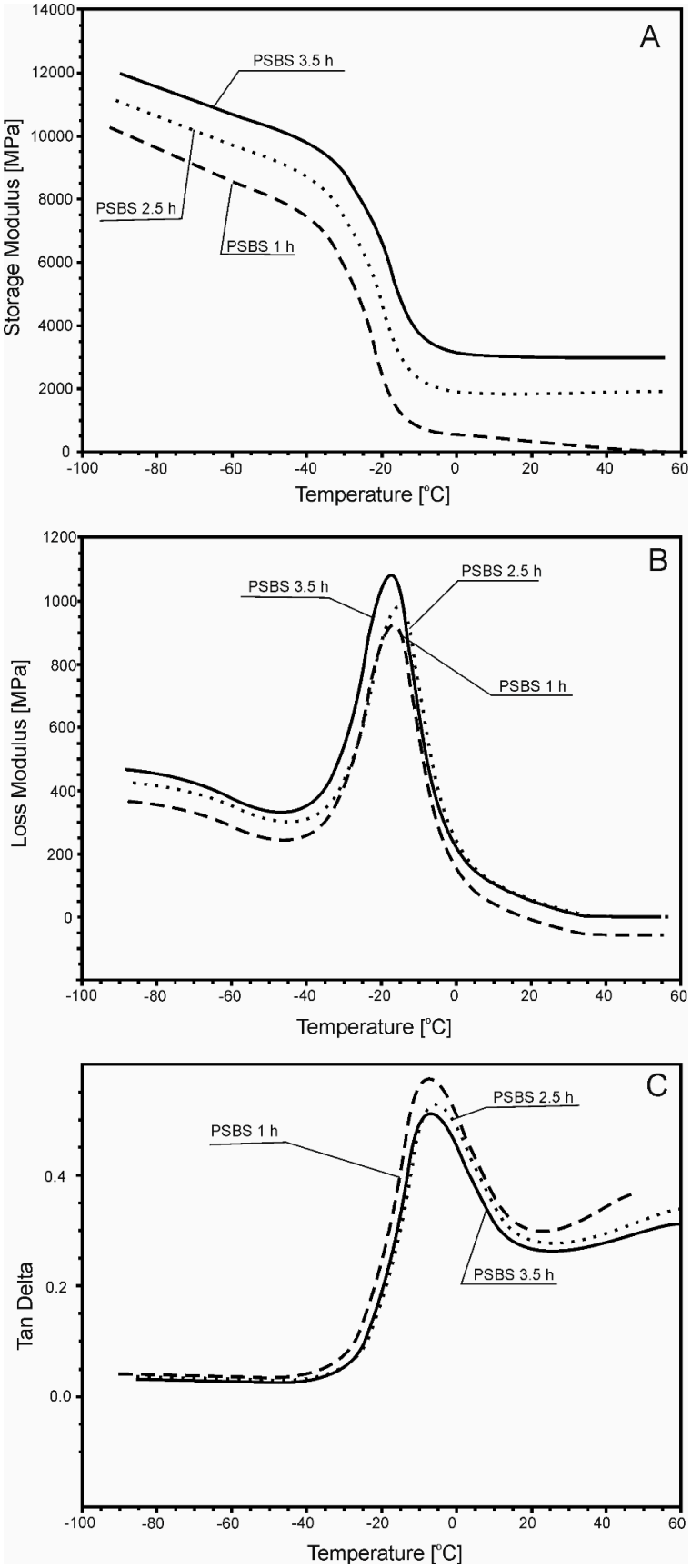

Figure 4. Storage modulus (E′) (**A**), loss modulus (E″) (**B**) and loss tangent (tan delta versus temperature) **(C)** for PSBS 1 h, PSBS 2.5 h and PSBS 3.5 h.

Three temperature ranges for the storage modulus can be observed. In the first temperature range (−100 °C to −40 °C), the storage modulus function does not show significant changes because polymers are in the glassy state. The initial value of the storage modulus for PSBS 3.5 h is significantly higher compared to its value for PSBS 2.5 h and PSBS 1 h. In the second temperature range (−40 °C to −10 °C), the value of the storage modulus decreases, which corresponds to a process of viscoelastic relaxation associated with the amorphous phase undergoing the glass-transition. In the third temperature range (0 °C to 50 °C), the storage modulus of PSBS 2.5 h and PSBS 3.5 h is constant, and a flexibility plateau can be observed. PSBS 1 h in the temperature range 0 °C to 50 °C exhibits the subservience of elastic to viscous properties and a rapid decline of the storage modulus. This phenomenon is not observed for PSBS 3.5 h and PSBS 2.5 h. The loss modulus E″ = f(T) and loss tangent tan delta = f(T) functions exhibit peak maximum corresponding to alpha relaxation. It is associated with the amorphous phase undergoing the glass-transition. The glass-transition temperature value measured by DMTA is 10 °C higher than the T_g value measured by DSC. Such discrepancy in results is typical for those methods.

3.4. Mechanical Properties

Figure 5 presents the results of tensile tests for PSBS after 1, 2.5, and 3.5 h polycondensation time.

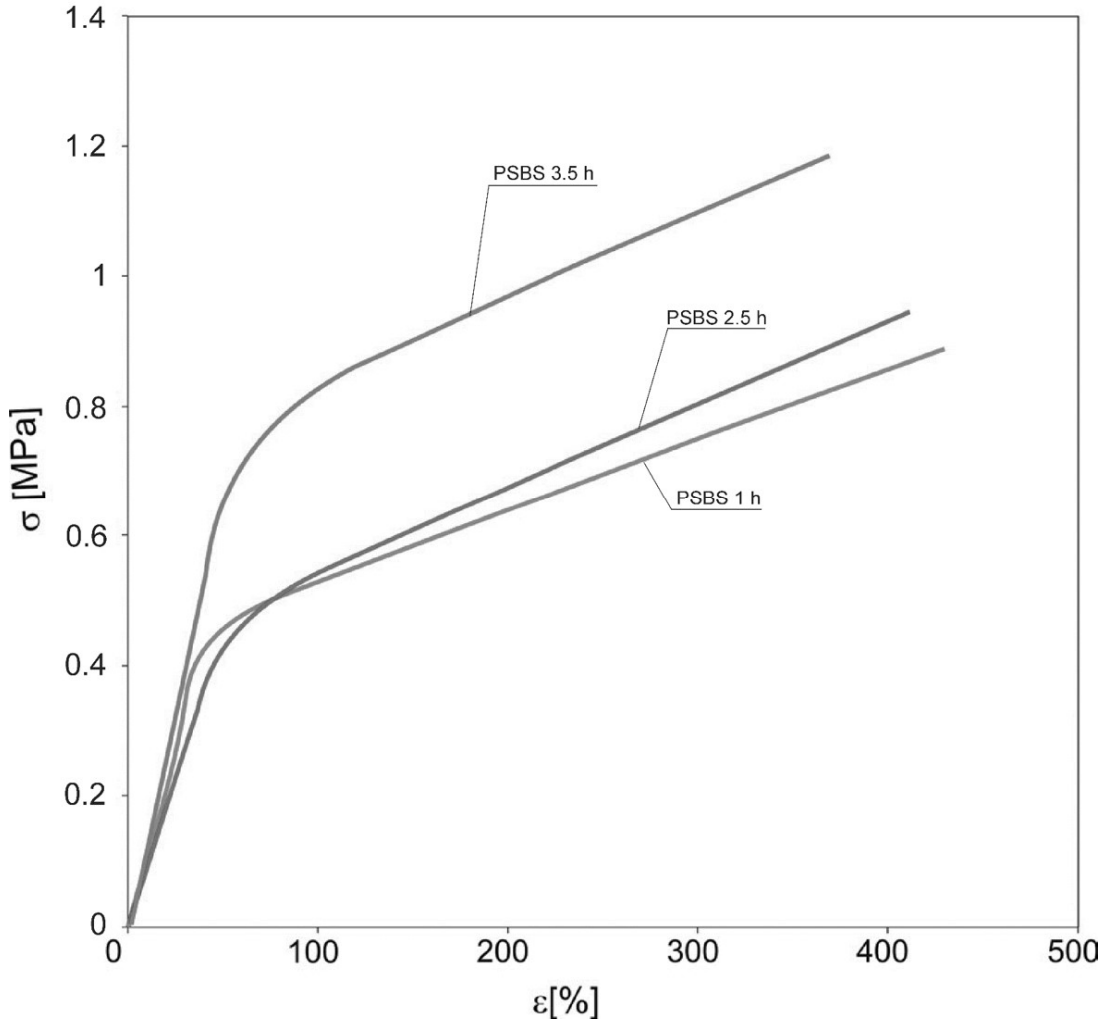

Figure 5. Mechanical properties of PSBS 1 h, PSBS 2.5 h and PSBS 3.5 h.

All obtained elastomers, regardless of polycondensation time, show the course of the stress–strain characteristic for elastomeric materials. It can be observed that the tensile stress increases with

increasing polycondensation time with a slight decrease in strain. PSBS 3.5 h shows a stress value of 1.2 MPa while maintaining a strain at 380%, which provides a good basis for qualifying this material as a competition for sorbitol-based materials described in the literature [11,12]. Higher tensile stress exhibited by PSBS 3.5 h correlates to DMTA results showing the highest storage modulus E' for this material.

3.5. Gel Fraction

The obtained elastomeric materials are characterized by a high degree of cross-linking, which can be observed in the gel fraction test. The results are presented in Figure 6.

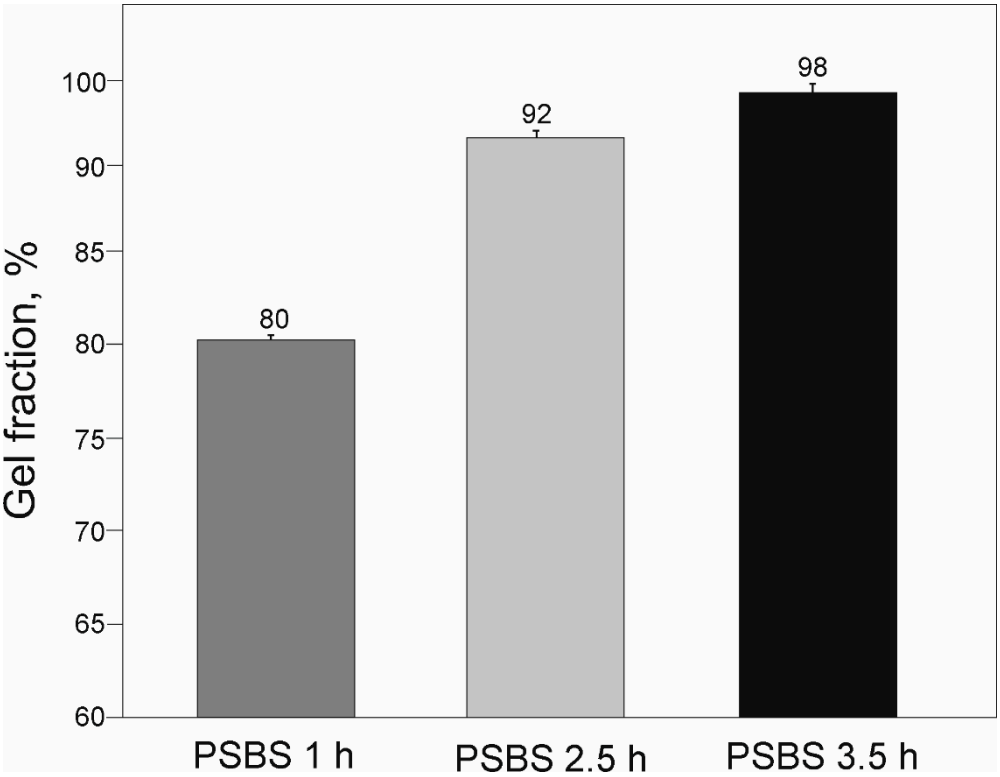

Figure 6. Gel fraction of PSBS 1 h, PSBS 2.5 h and PSBS 3.5 h.

The expected effect was the increase of gel fraction along with the polycondensation time. For PSBS 1 h, the value of the gel fraction is 80%, 92% for PSBS 2.5 h, and 98% for PSBS 3.5 h. These results correspond very well with thermal and mechanical results. The highest gel fraction of PSBS 3.5 h correlates with the best mechanical properties shown by mechanical tests and the highest content of the amorphous phase shown by both DSC and DMTA and confirms that 3.5 h of polycondensation time is the best option for synthesizing such materials.

3.6. ^{1}H Nuclear Magnetic Resonance Spectroscopy (NMR)

In order to confirm the structure of the PSBS copolymer, ^{1}H NMR analysis (Figure 7) was performed. The peak at about 1.30 ppm was due to a CH_2(c) group doublet at 1.62, and the 1.71 ppm was connected to CH_2(b) and CH_2 (g) groups; the peak at about 2.32 ppm was attributed to a CH_2 (a) group. The peak at about 4.09 ppm was assigned to the proton next to the oxygen atom, which is a part of the ester bond between sebacic acid and butylene glycol. The peak at about 4.23 ppm is due to the proton next to the oxygen atom, which is a part of the ester bond between sebacic acid and sorbitol. Peaks between about 4.02 ppm and 3.56 ppm are connected to CH_2(d) groups in sorbitol.

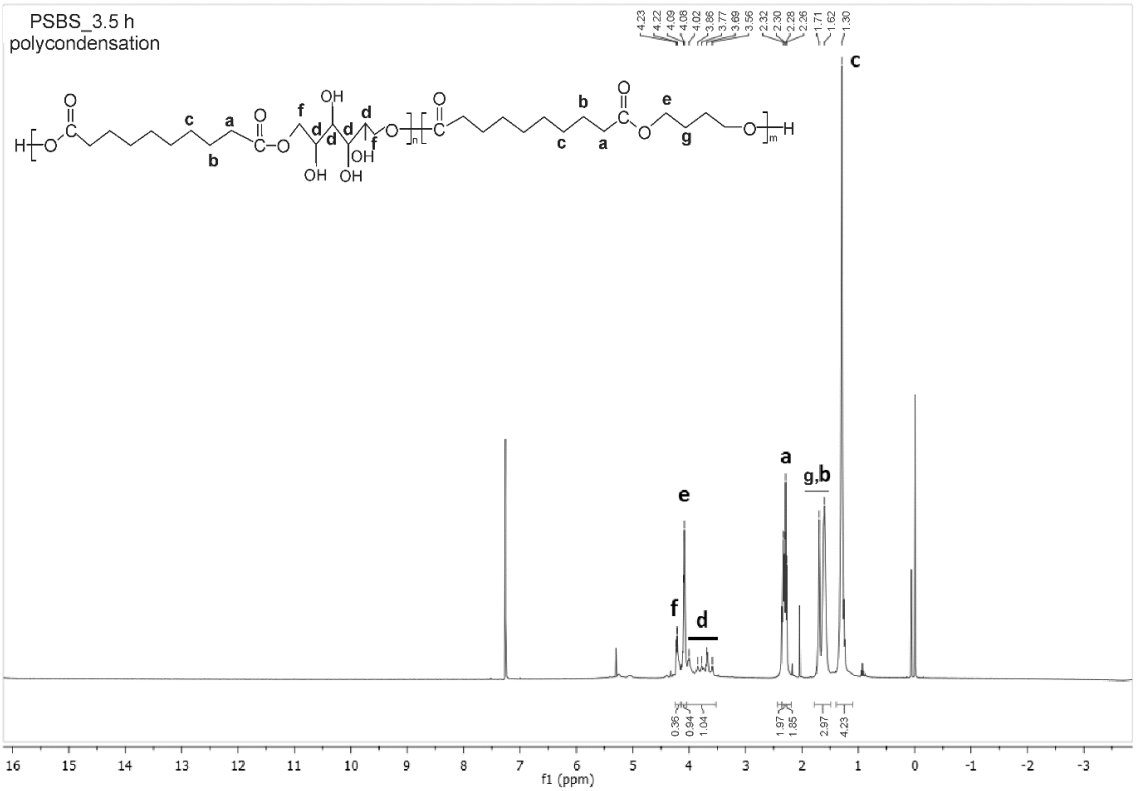

Figure 7. NMR analysis of PSBS 3.5 h.

4. Conclusions

Materials based on butylene glycol, sebacic acid and sorbitol monomers were obtained. Three different polycondensation times were used. Thermal and mechanical properties and gel fraction were tested. The results confirm that utilizing a 3.5 h polycondensation time leads to obtaining materials with the best properties, due to its highest cross-linking degree. Results obtained from different methods correlate well with each other. High gel fraction, thermal stability and good mechanical properties of PSBS elastomers suggest possible industrial applications.

Author Contributions: M.P.-H., K.B., J.P. conceived, designed and performed the experiment, analysed the data and wrote the paper. All authors have read and agreed to the published version of the manuscript.

Funding: This research received no external funding.

Conflicts of Interest: The authors declare no conflict of interest.

References

1. Neeley, W.L.; Redenti, S.; Klassen, H.; Tao, S.; Desai, T.; Young, M.J.; Langer, R. A microfabricated scaffold for retinal progenitor cell grafting. *Biomaterials* **2008**, *29*, 418–426. [CrossRef] [PubMed]
2. Sun, Z.J.; Chen, C.; Sun, M.Z.; Ai, C.H.; Lu, X.L.; Zheng, Y.F.; Yang, B.F.; Dong, D.L. The application of poly (glycerol-sebacate) as biodegradable drug carrier. *Biomaterials* **2009**, *30*, 5209–5214. [CrossRef] [PubMed]
3. Zaky, S.H.; Lee, K.W.; Gao, J.; Jensen, A.; Verdelis, K.; Wang, Y.; Almarza, A.J.; Sfeir, C. Poly (glycerol sebacate) elastomer supports bone regeneration by its mechanical properties being closer to osteoid tissue rather than to mature bone. *Acta Biomater.* **2017**, *54*, 95–106. [CrossRef] [PubMed]
4. Chen, Q.Z.; Bismarck, A.; Hansen, U.; Junaid, S.; Tran, M.Q.; Harding, S.E.; Ali, N.N.; Boccaccini, A.R. Characterisation of a soft elastomer poly(glycerol sebacate) designed to match the mechanical properties of myocardial tissue. *Biomaterials* **2008**, *29*, 47–57. [CrossRef]
5. Motlagh, D.; Yang, J.; Lui, K.Y.; Webb, A.R.; Ameer, G.A. Hemocompatibility evaluation of poly(glycerol-sebacate) in vitro for vascular tissue engineering. *Biomaterials* **2006**, *27*, 4315–4324. [CrossRef]

6. Bettinger, C.J.; Orrick, B.; Misra, A.; Langer, R.; Borenstein, J.T. Microfabrication of poly (glycerol-sebacate) for contact guidance applications. *Biomaterials* **2006**, *27*, 2558–2565. [CrossRef]
7. Kemppainen, J.M.; Hollister, S.J. Tailoring the mechanical properties of 3D-designed poly(glycerol sebacate) scaffolds for cartilage applications. *J. Biomed. Mater. Res. Part A* **2010**, *94*, 9–18. [CrossRef]
8. Rosenbalm, T.N.; Teruel, M.; Day, C.S.; Donati, G.L.; Morykwas, M.; Argenta, L.; Kuthirummal, N.; Levi-Polyachenko, N. Structural and mechanical characterization of bioresorbable, elastomeric nanocomposites from poly(glycerol sebacate)/nanohydroxyapatite for tissue transport applications. *J. Biomed. Mater. Res. Part B Appl. Biomater.* **2016**, *104*, 1366–1373. [CrossRef]
9. Liang, S.L.; Cook, W.D.; Thouas, G.A.; Chen, Q.Z. The mechanical characteristics and in vitro biocompatibility of poly(glycerol sebacate)-Bioglass® elastomeric composites. *Biomaterials* **2010**, *31*, 8516–8529. [CrossRef]
10. Sundback, C.A.; Shyu, J.Y.; Wang, Y.; Faquin, W.C.; Langer, R.S.; Vacanti, J.P.; Hadlock, T.A. Biocompatibility analysis of poly(glycerol sebacate) as a nerve guide material. *Biomaterials* **2005**, *26*, 5454–5464. [CrossRef]
11. Kumar, A.; Kulshrestha, A.S.; Gao, W.; Gross, R.A. Versatile route to polyol polyesters by lipase catalysis. *Macromolecules* **2003**, *36*, 8219–8221. [CrossRef]
12. Bruggeman, J.P.; de Bruin, B.J.; Bettinger, C.J.; Langer, R. Biodegradable poly(polyol sebacate) polymers. *Biomaterials* **2008**, *29*, 4726–4735. [CrossRef] [PubMed]
13. Barrett, D.G.; Yousaf, M.N. Thermosets synthesized by thermal polyesterification for tissue engineering applications. *Soft Matter* **2010**, *6*, 5026–5036. [CrossRef]
14. Kavimani, V.; Jaisankar, V. Synthesis and Characterisation of Sorbitol Based Copolyesters for Biomedical Applications. *J. Phys. Sci. Appl.* **2014**, *4*, 507–515.
15. Piątek-hnat, M. Influence of the addition of citric acid on the physico-chemical properties of poly(sorbitol sebacate-co- butylene sebacate). *Int. J. Sci. Eng. Res.* **2018**, *9*, 1092–1094.
16. Lee, S.H.; Shin, S.R.; Lee, D.S. Sorbitol as a chain extender of polyurethane prepolymers to prepare self-healable and robust polyhydroxyurethane elastomers. *Molecules* **2018**, *23*, 2515. [CrossRef]
17. Tham, W.H.; Wahit, M.U.; Kadir, M.R.A.; Wong, T.W. Mechanical and thermal properties of biodegradable hydroxyapatite/poly(sorbitol sebacate malate) composites. *Songklanakarin J. Sci. Technol.* **2013**, *35*, 57–61.
18. Bruggeman, J.P.; Bettinger, C.J.; Langer, R. Biodegradable xylitol-based elastomers: In vivo behavior and biocompatibility. , *J. Biomed. Mater. Res. Part A* **2010**, *95*, 92–104. [CrossRef]
19. Bruggeman, J.P.; Bettinger, C.J.; Nijst, C.L.E.; Kohane, D.S.; Langer, R. Biodegradable xylitol-based polymers. *Adv. Mater.* **2008**, *20*, 1922–1927. [CrossRef]
20. Deepa, K.; Jaisankar, V. A Study on Xylitol Based Copolyester for In vitro Degradation Applications. *Int. J. Chem. Technol. Res.* **2018**, *11*, 69–76. [CrossRef]
21. Hu, J.; Gao, W.; Kulshrestha, A.; Gross, R.A. "Sweet polyesters": Lipase-catalyzed condensation-polymerizations of alditols. *ACS Symp. Ser.* **2008**, *999*, 275–284.
22. Moorhoff, C.; Li, Y.; Cook, W.D.; Braybrook, C.; Chen, Q.Z. Characterization of the prepolymer and gel of biocompatible poly(xylitol sebacate) in comparison with poly(glycerol sebacate) using a combination of mass spectrometry and nuclear magnetic resonance. *Polym. Int.* **2015**, *64*, 668–688. [CrossRef]
23. Sonseca, Á.; Camarero-Espinosa, S.; Peponi, L.; Weder, C.; Foster, E.J.; Kenny, J.M.; Giménez, E. Mechanical and shape-memory properties of poly(mannitol sebacate)/cellulose nanocrystal nanocomposites. *J. Polym. Sci. Part A Polym. Chem.* **2014**, *52*, 3123–3133. [CrossRef]
24. Selvam, S.; Pithapuram, M.V.; Victor, S.P.; Muthu, J. Injectable in situ forming xylitol-PEG-based hydrogels for cell encapsulation and delivery. *Colloids Surfaces B Biointerfaces* **2015**, *126*, 35–43. [CrossRef]
25. Li, Y.; Thouas, G.A.; Chen, Q. Novel elastomeric fibrous networks produced from poly(xylitol sebacate)2:5 by core/shell electrospinning: Fabrication and mechanical properties. *J. Mech. Behav. Biomed. Mater.* **2014**, *40*, 210–221. [CrossRef]
26. Li, Y.; Chen, Q.Z. Fabrication of mechanically tissue-like fibrous poly(xylitol sebacate) using core/shell electrospinning technique. *Adv. Eng. Mater.* **2015**, *17*, 324–329. [CrossRef]
27. Firoozi, N.; Kang, Y. A Highly Elastic and Autofluorescent Poly(xylitol-dodecanedioic Acid) for Tissue Engineering. *ACS Biomater. Sci. Eng.* **2019**, *5*, 1257–1267. [CrossRef]

28. Akiyama, H.; Yoshida, M. Photochemically reversible liquefaction and solidification of single compounds based on a sugar alcohol scaffold with multi azo-arms. *Adv. Mater.* **2012**, *24*, 2353–2356. [CrossRef]
29. Sugane, K.; Takahashi, H.; Shimasaki, T.; Teramoto, N.; Shibata, M. Stereocomplexation, Thermal and Mechanical Properties of Conetworks Composed of Star-Shaped L-Lactide, D-Lactide and ε-Caprolactone Oligomers Utilizing Sugar Alcohols as Core Molecules. *Polymers* **2017**, *9*, 582. [CrossRef]